Rock fabric and microseismic: an integrated approach

Martin Haege*, Schlumberger, Stavanger, Norway
mhaege@slb.com
and
Shawn Maxwell, Schlumberger, Calgary, Canada
Lars Sonneland, Schlumberger, Stavanger, Norway
Mark Norton, Progress Energy Resources, Calgary, Canada

Summary

This paper presents a new approach where subtle discontinuities mapped on 3D reflection seismic are integrated with the microseismic information from three multi-stage hydraulic stimulations. Regions with a high degree of rock fabric correlate with microseismic events with a high seismic moment and a tectonic b-value of around 1. Fracture complexity increases as a result of changing rock properties and/or perturbations of in-situ stresses in areas with a high degree of rock fabric. The differing production behavior between the three wells could be explained by the changing degree of rock fabric.

Introduction

Microseismic monitoring has become a standard technique to monitor fracture propagation during hydraulic fracture stimulation. Shales are texturally anisotropic rocks with varying diagenetic histories and mineralogical content, often leading to complex fracture networks. Dissimilarities in fracture evolution and large variations in production are commonly observed within a short interval along lateral treatment wells. The factors responsible for this variability are still poorly understood. Besides local stress variations and rock properties, pre-existing faults and zones of weakness in the rock are assumed to play a major role. Pre-existing faults can result in inefficient reservoir stimulation e.g. by guiding hydraulic fractures into water-bearing zones, therefore detailed knowledge about the fault network is essential.

This study integrates 3D reflection seismic with passive seismic. Currently there is great interest in combining these two geophysical methods to improve reservoir characterization (e.g. Keller *et al.*, 2009; Rich and Ammerman 2010; Hayles *et al.*, 2011). Small scale discontinuities called rock fabric are derived from 3D reflection seismic and investigated. Rock fabric is at the limit of seismic resolution which makes mapping a challenging task. A new vector attribute is introduced and applied to capture the rock fabric from 3D reflection seismic data. It is being evaluated to what extent seismic moment and microseismic event location (determined from hydraulic fracture monitoring) can be correlated with rock fabric observations from 3D reflection seismic. The uncertainties in this relationship are discussed. The overall aim is to improve the understanding of unconventional reservoirs. We will use the term 'rock fabric' for pre-existing zones of weakness in the rock and the term 'fractures' for hydraulically induced fractures through stimulation.

Mapping rock fabric

Manual mapping of faults is a time-consuming task. Automatic tools and workflows are commonly used to highlight and extract faults in order to reduce interpretation time and increase objectivity. A typical workflow for fault extraction consists of seismic conditioning, attribute computation, enhancement of faults and extraction of fault patches (Figure 1). Each step of the workflow is a challenging task and still subject to extensive research in the industry. The step 'enhancement of faults' increases the signal

(faults) to noise ratio by suppressing small features (highlighted by the red circles in Figure 1). This is essential when mapping large scale faults, however, important information about rock fabric is lost in this step. This study focuses on the seismic attribute in order to retain as much information as possible.
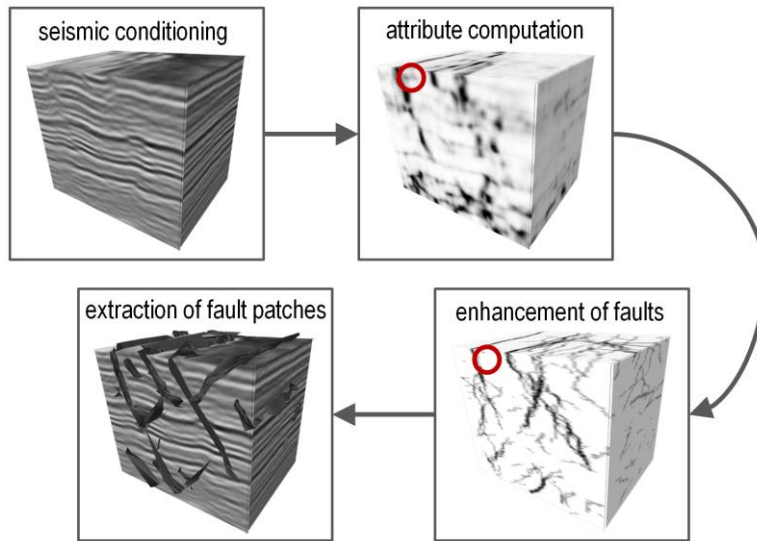

Figure 1: Typical workflow for mapping faults. Red circles highlight reduction of information from the step 'attribute computation' to 'enhancement of faults'.

A new seismic vector attribute was applied which detects abrupt spatial changes in the 3D normal vector field. A polynomial reconstruction of the seismic traces allows an analytical representation with sub-seismic resolution. The normal vectors are computed by the gradient field of the seismic cube by calculation of the partial derivatives. Horizons with sub-sample precision may be extracted from the extrema points (extrema on the seismic correspond to zero crossings on the time derivative) (Figure 2a) (Borgos *et al.*, 2006). The magnitude of the rotation of the 3D normal vector field captures subtle changes in seismic reflections and hence subtle changes in the imaged subsurface rocks (Figure 2b). This vector attribute will consequently enable mapping of subtle changes in rock fabric.
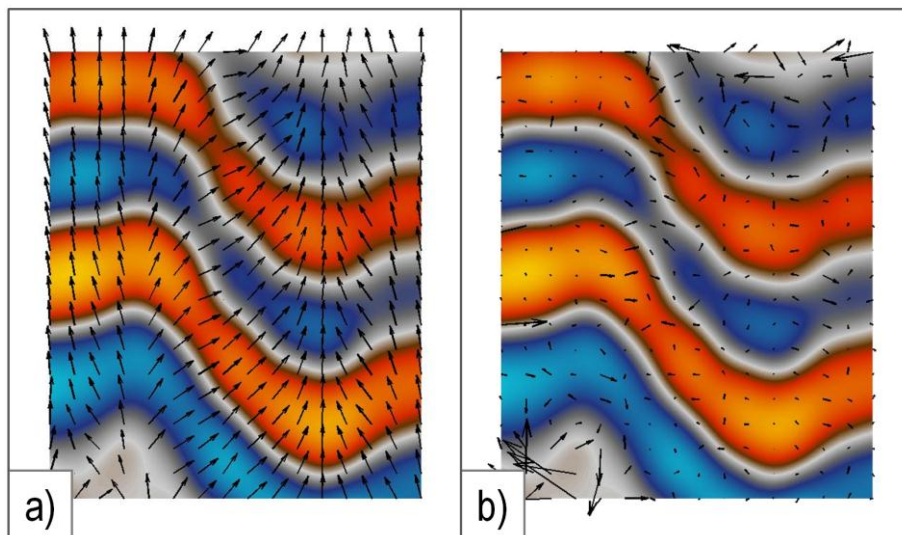

Figure 2: Vectors overlaid on a vertical seismic section. a) normal vector field b) rotation vectors, weighted by the magnitude of the rotation of the 3D normal vector field.

Uncertainties

There are uncertainties involved when comparing information observed on 3D reflection seismic with information derived from passive seismic. Different velocity models may have been used in processing, i.e. for the migration of 3D reflection seismic and for microseismic event location. In addition there are uncertainties in microseismic event location due to unfavorable source-receiver distance or poor receiver coverage etc. Another source of uncertainty is resolution or scaling. Microseismic events recorded during hydraulic stimulation have a source radius typically less than 10 m, this may be at the limit of the 3D reflection seismic resolution which makes comparison a challenging task. Further, the 3D reflection seismic could be affected by acquisition footprints which could lead to biased fault illumination. To account for such spatial uncertainties the seismic vector attribute cube has been smoothed with a Gaussian filter, a compromise between honoring uncertainties and retaining detail.

Case study

Microseismic data was available from three horizontal multi-stage hydraulic stimulations within the Upper Montney Formation in NE British Columbia, Canada (Well A, B and C in Figure 3). The target interval consists of fine to very fine grained siltstone with permeabilities between 0.001 to 0.05 mD, porosities between 3-6% and is approximately 1750 m TVD. In order to have a uniform data set unbiased by the distance dependent detection threshold only the nearest stages to the monitoring well were taken into account (10 out of 21 stages). The magnitude of completeness (M_C) was determined to M_W -2.2 and events with a smaller M_C were removed from the catalogue; around 1000 events remained for further analysis (Maxwell *et al.*, 2011a).

Observations

The relationship between microseismic events and large faults has been discussed by Maxwell *et al.* (2011b).

The smoothed seismic attribute cube containing the magnitude of the rotation of the 3D normal vector field was used to investigate a possible correlation between microseismic events with a high seismic moment and areas with a high degree of rock fabric. The seismic attribute values were mapped onto the microseismic events. Figure 3a displays the microseismic event set colored by rock fabric, with the darker colors corresponding to higher degrees of rock fabric. Magnitudes are indicated by the size of the points with larger points representing higher magnitudes. Significant differences in the microseismic response were observed (the termination of microseismic events towards NE may be attributed to a large fault system (Maxwell *et al.* 2011b)). In general, the induced seismicity around Well A and Well B indicates fractures oriented perpendicular to the least principal stress direction, whereas the fractures around Well C tend to be scattered and heterogeneous in shape. The area in the SE around Well C shows a concentration of microseismic events with a high degree of rock fabric. This suggests reactivation of pre-existing zones of weakness in the rock in this region.

It is important to consider the general trend rather than single events due to the uncertainties discussed. A density map of the rock fabric was calculated for this purpose with the area divided into 15 by 15 cells with each cell having the cumulative sum of the attribute values calculated. Figure 3b displays the result and shows a high degree of rock fabric concentration in the SE.
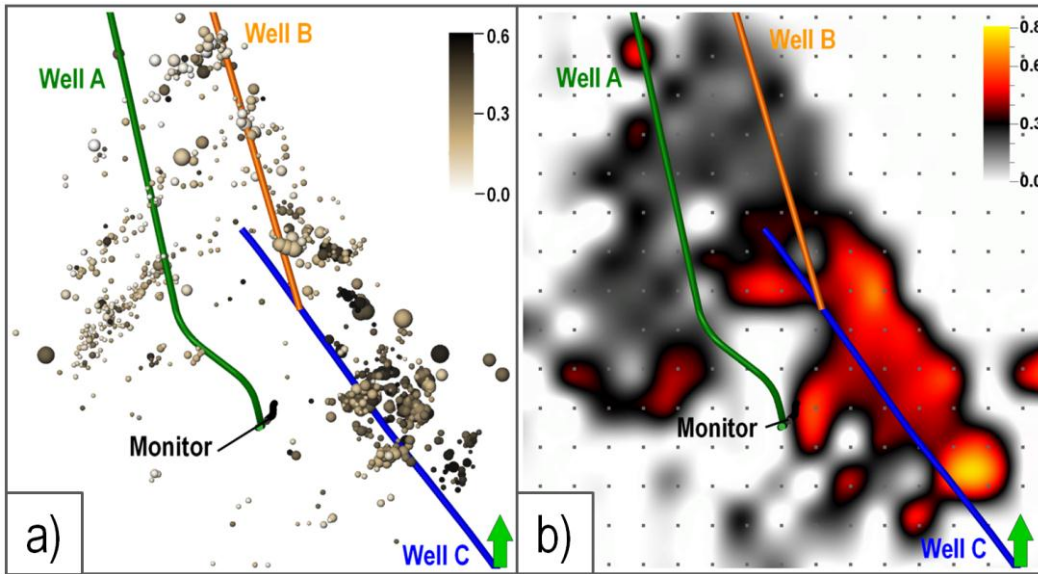
Figure 3: Top view of monitor well and three horizontal treatment wells A, B and C. a) Microseismic events sized by magnitude and colored by the seismic attribute value. Dark colors represent high degree of rock fabric. N-S extend is about 1600 m. b) Density map of the rock fabric. Centers of bins are indicated by grey points.

Reactivation of pre-existing faults typically produces higher magnitude events and tends to have a tectonic b-value of around 1, whereas hydraulically induced fractures are typically accompanied by low magnitude events exhibiting a higher b-value (Maxwell *et al.*, 2009; Downie *et al.*, 2010; Wessels *et al.*, 2011). For the same microseismic data set Maxwell *et al.* (2011a) calculated a contour map of the b-value as well as a contour map of the logarithm of seismic moment density (Figure 4).

By comparing Figures 3 and 4 a correlation between areas with a high seismic moment, b-value around 1 and a high degree of rock fabric can be observed. Regions with a low degree of rock fabric can be correlated with low magnitude events and a high b-value.
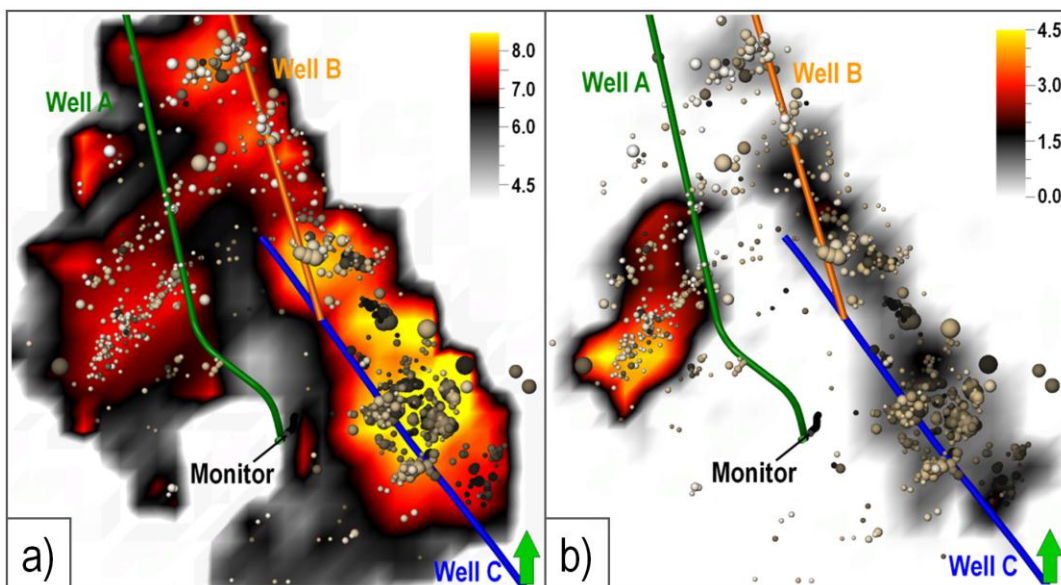

Figure 4: Microseismic events sized by magnitude and colored by degree of rock fabric overlaid on a) Contour map of logarithm of seismic moment. b) Contour map of b-value slope of magnitude-frequency relationship (after Maxwell *et al.* (2011a)).

Areas exhibiting a low Poisson ratio (PR) are associated with an enhanced relative production. Norton *et al.* (2010) performed AVO analysis and inverted for elastic properties for the data set. Figure 5a shows the minimum PR map for the interval of interest in which the majority of the microseismic events occurred. Well A and B are situated in low PR regions and Well C is at the transition zone between low PR to the SW and high PR to the NE. Microseismic events sized by magnitude have been overlaid. For the same interval a rock fabric map was created and the mean seismic attribute value for each seismic trace in the interval of interest was calculated (Figure 5b).
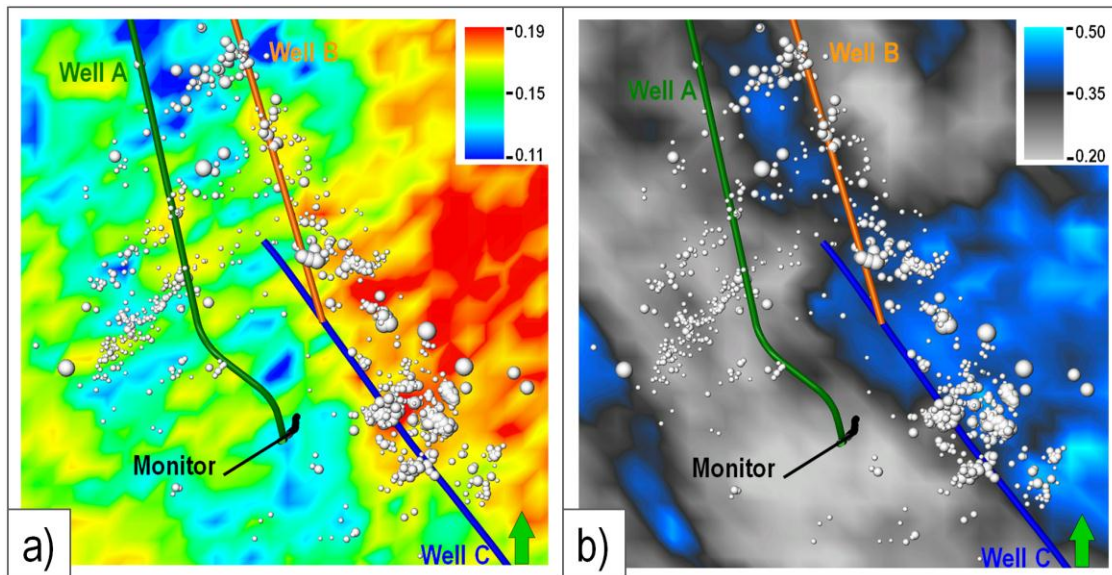

Figure 5: Microseismic events sized by magnitude overlaid on a) Minimum PR (after Norton *et al.* (2010)). b) Mean rock fabric. Blue colors represent high degree of rock fabric.

To the NE of Well C a high PR and high degree of rock fabric is observed. In an isotropic medium low PR is associated with low horizontal stresses making these areas preferable for fracture propagation. This is observed for the microseismic events around Well A, B and for a few small magnitude events SW of Well C. However, the majority of microseismic events around Well C did not occur towards the SW in the low PR region, they are rather concentrated in the area of high PR and high degree of rock fabric.

Horizontal stress ratio is assumed to determine fracture growth. High stress anisotropy leads to planar fractures and low stress anisotropy to a complex interacting fracture development (Wikel, 2011). Complex fracture networks tend to create a larger area of reservoir contact which is essential for production optimization. A general high horizontal stress ratio might be perturbed locally by the presence of a high degree of rock fabric. The fracture behavior around Well C may therefore be explained by a complex interaction of in-situ stress perturbation and/or change in rock properties and rock fabric. This also might explain the relatively high production rate and the relatively steep initial pressure decline observed on Well C (Maxwell *et al.*, 2011a).

Implications

Using the information of rock fabric (in combination with other observations such as stress information, TOC etc.) may assist fracture engineering design and contribute to more intelligent completions. Detailed knowledge of spatial rock fabric distribution may also help adjust real-time stimulation in order to prevent out of zone fracturing. To enable this, each microseismic event is taken as a seed point and patches are then extracted in areas with a high degree of rock fabric. The search volume is guided by the location uncertainty and the seismic moment which is a function of the source radius (Figure 6).
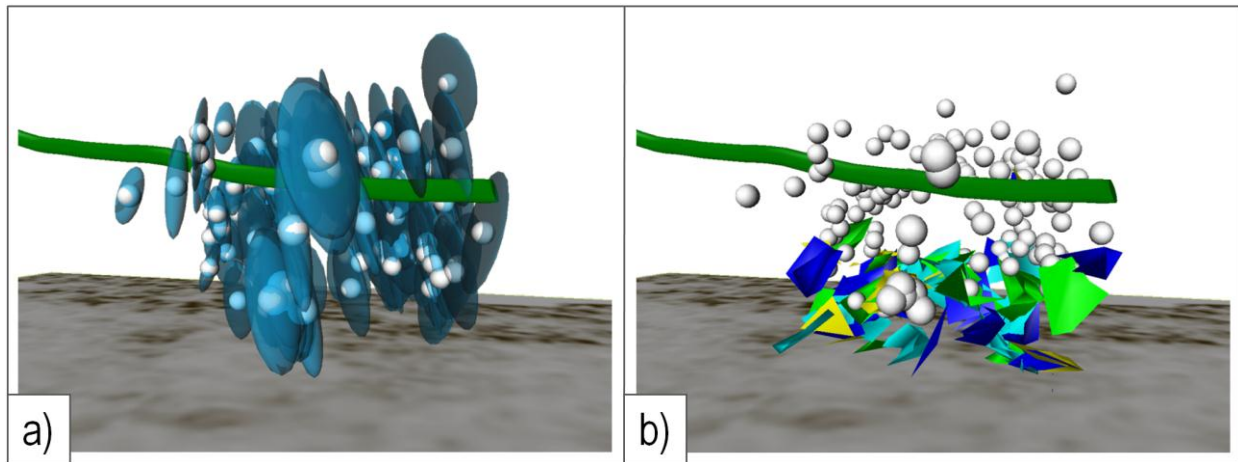
Figure 6: a) Microseismic events with uncertainty ellipsoids b) Patches indicate areas with a high degree of rock fabric.

Conclusions

Understanding the behavior of fractures induced by hydraulic stimulation is essential to optimize production. Fracture propagation is mainly influenced by in-situ stresses, rock properties and pre-existing faults. Beside large scale faults, subtle zones of weakness in the rock (rock fabric) play an important role which is the focus of this study. A methodology has been demonstrated how rock fabric can be mapped on 3D reflection seismic and can be integrated with results from passive microseismic monitoring. A new seismic vector attribute was introduced and applied to map subtle discontinuities in the subsurface rock providing high level of detail of the rock's heterogeneity. Smoothing of the seismic attribute accounts for the uncertainties when combining the 3D reflection seismic with the passive seismic. Fracture complexity and seismic moment correlate to rock fabric.

Acknowledgements

References

Borgos, H. G., O. Gramstad, G. V. Dahl, P. Le Guern, L. Sonneland, and J. F. Rosalba, 2006, Extracting horizon patches and geo-bodies from 3D seismic waveform sequences: Annual Meeting, SEG, Expanded Abstracts, 1595-1599.

Downie, R. C., E. Kronenberger, and S. C. Maxwell, 2010, Using Microseismic Source Parameters to Evaluate the Influence of Faults on Fracture Treatments – A Geophysical Approach to Interpretation: SPE 134772.

Hayles, K., R. L. Horine, S. Checkles, and J. P. Blangy, 2011, Comparison of microseismic results from the Bakken Formation processed by three different companies: Integration with surface seismic and pumping data: Annual Meeting, SEG, Expanded Abstracts, 1468-1472.

Keller, W. R., B. J. Hulsey, and P. Duncan, 2009, Correlation of surface microseismic event distribution to water production and faults mapped on 3D seismic data: a West Texas case study: Annual Meeting, SEG, Expanded Abstracts, 1524-1526.

Maxwell, S. C., M. Jones, R. Parker, S. Miong, S. Leaney, D. Dorval, D. D'Amico, J. Logel, E. Anderson, and K. Hammermaster, 2009, Fault Activation During Hydraulic Fracturing: Annual Meeting, SEG, Expanded Abstracts, 1552- 1556.

Maxwell, S. C., D. Cho, T. Pope, M. Jones, C. Cipolla, M. Mack, F. Henery, M. Norton, and J. Leonard, 2011a, Enhanced Reservoir Characterization Using Hydraulic Fracture Microseismicity: SPE 140449.

Maxwell, S. C., T. Pope, C. Cipolla, M. Mack, L. Trimbitasu, M. Norton, and J. Leonard, 2011b, Understanding Hydraulic Fracture Variability Through Integrating Microseismicity and Seismic Reservoir Characterization: SPE 144207.

Norton, M., W. Hovdebo, D. Cho, M. Jones, and S. Maxwell, 2010, Surface seismic to microseismic: An integrated case study from exploration to completion in the Montney shale of NE British Columbia, Canada: Annual Meeting, SEG, Expanded Abstracts, 2095-2099.

Rich, J. P., and M. Ammerman, 2010, Unconventional Geophysics for Unconventional Plays: SPE 131779.

Wessels, S. A., A. De La Peña, M. Kratz, S. Williams-Stroud, and T. Jbeili, 2011, Identifying faults and fractures in unconventional reservoirs through microseismic monitoring: First Break, **29**, 99-104.

Wikel, K., 2011, Geomechanics: bridging the gap from geophysics to engineering in unconventional reservoirs: *First Break*, **29**, 71-80.